

Effect of Backfill on Wrap Faced Reinforced Soil Wall Subjected to Seismic Excitation

Arup Bhattacharjee¹, A.M.Krishna²

Asst. Professor, Dept. Of Civil Engg, Jorhat Engineering College, Jorhat, Assam, India¹

Asst. Professor, Dept. Of Civil Engg, Indian Institute of Technology, Guwahati, Assam, India²

Abstract— Reinforced soil walls offer excellent solution to many problems associated with earth retaining structures especially under seismic conditions. This paper present the seismic response of wrap faced reinforced soil retaining walls through numerical models. Numerical models of the wrap faced reinforced soil walls are simulated using FLAC3D. Backfill soil is modeled as elasto-plastic Mohr Coulomb material model coded with stress dependent hyperbolic soil modulus model under static loading and non-linear hysteretic constitutive model that follows the Massing rule, under cyclic loading. The reinforcement is modeled as geogrid shell structural element. Various interfaces are also considered for proper interaction between dissimilar elements. The effects of backfill friction angle and dilation angle on the failure modes are being studied. It is observed that the deformation of wrap faced wall subjected to dynamic excitation consist of three different modes of failure: shear deformation within reinforced zone, relative compaction near end of reinforcement and compound failure surface extending to backfill zone.

Keywords—Reinforced soil wall, Wrap faced wall, seismic excitation, FLAC^{3D}, Massing rule, Hysteric behavior, Octahedral shear strain

I. INTRODUCTION

The reinforced soil retaining structure often referred as Mechanically Stabilized Earth (MSE) structures have many qualities like aesthetic, reliability, low cost, impressive seismic performance and ability to withstand large deformations without structural distress. The

reinforced soil retaining structure has three main components: backfill, reinforcement and facing element. Reinforcement may be metal strips or polymer products like geotextile, geogrid, geomembrane etc. Wall facing system may be: wrap facing, full height rigid facing, segmental block facing and modular block facing. The studies on seismic behavior of reinforced soil walls has been the interest of many researchers that can be classified into three categories: experimental studies mainly based on shake table and centrifuge tests, analytical model studies based on pseudo-static and pseudo-dynamic approach, and numerical model studies. Finite element or finite difference methods are used for numerical modeling. Hatami and Bathurst (2000) studied the influence of structural design on the fundamental frequency of the reinforced soil walls by FLAC. Recently Ling et al. (2010), Liu et al. (2011) and Liu and Ling (2011) used finite element procedure to study the behavior of reinforced soil walls. Krishna and Latha (2012) modeled dynamic response of wrap faced retaining wall using FLAC. In this paper, a calibrated model (Bhattacharjee and Krishna, 2012) is considered and the effects of backfill soil and reinforcement are analysed in terms of strains, horizontal displacements and vertical settlement.

II. GENERATION OF NUMERICAL MODEL FOR WRAP FACED WALL

The numerical simulation of full scale model developed by Bhattacharjee and Krishna (2012) are adopted in the present study. A full scale model of size 6 m high, 18 m long and 1 m wide with four layers of reinforcement is considered for study of seismic

behavior. The foundation of wall is considered to be rigid and no vertical displacements are allowed. The wrap faced walls are constructed in sequence of equal layers. Each layer is wrapped around with structural elements which represent the geotextiles. The whole grid is divided into cubical brick elements of size 25 cm each. The size of grid are selected in such a way that , the mesh size of the model must be approximately smaller than one-tenth to one-eighth of the highest frequency component of the input wave for accurate transmission of wave through a model (Kuhlemeyer and Lysmer, 1973) during dynamic shaking. Before placing the first layer of back fill, the foundation zone is generated and brought to static equilibrium. The model is generated in equal lifts with reinforcement wrapped around to form facing for each lift. The facing of the model is fixed in x direction to represent the facing support. The model is solved for static equilibrium after generation of grids of each lift. The supports are removed in sequence from top to bottom after building the wall up to full height and applying the surcharge pressure of 5 kPa. After support removal of each lift the model is solved for static equilibrium.

III. MATERIAL PROPERTIES

Backfill Material

The backfill soil is modelled as elasto-plastic Mohr Coulomb material model coded with hyperbolic soil modulus model proposed by Duncun et al. (1980). During the construction stages, the soil layer is placed layer by layer. So confining pressure on each zone change with increase in height of fill. The modulus of granular soil increases with increase in confining pressure. This effect of changing soil modulus with confining pressure during construction is applied by modified hyperbolic soil modulus model (Duncun et al. 1980). The deformation modulus (E_t) expressed by the Duncun hyperbolic equation is

$$E_t = \left[1 - \frac{R_f(1-\sin\phi)(\sigma_1-\sigma_3)}{2c\cos\phi+2\sigma_3\sin\phi} \right]^2 K \times p_a \left(\frac{\sigma_3}{p_a} \right)^2 \quad (1)$$

where K is the modulus number; n is the modulus exponent; c is the cohesion; σ_1 and σ_3 are the major and minor effective confining stress respectively; ϕ is the angle of internal friction; R_f is the failure ratio; p_a is atmospheric pressure. A small cohesion value is applied

to prevent premature yielding (Hatami and Bathurst, 2005). The FLAC^{3D} has built in Mohr-Coulomb constitutive model. But the hyperbolic model can be incorporated by FISH subroutines that update the soil modulus according to their stress condition.

The use of constant shear modulus during dynamic loading is not appropriate due to cyclic nature of soil. The shear behavior of granular soils under cyclic loading is modeled using non-linear and hysteretic constitutive relation that follows the Massing rule (Cai and Bathurst, 1995) during unloading and reloading cycles (Fig. 1).

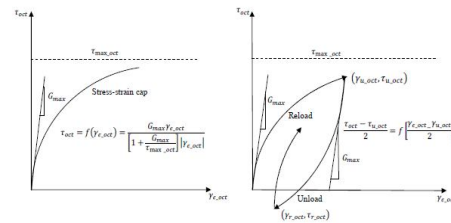


FIG. 1 NONLINEAR STRESS-STRAIN MODEL OF GRANULAR SOIL (A) STRESS-STRAIN CAP (B) UNLOAD-RELOAD (AFTER CAI & BATHURST 1995)

In this model, the shear modulus is determined on the basis of stress and strain states that may vary considerably during simulation runs. The tangent shear modulus during the first cycle is expressed as

$$G_t = \frac{G_{max}}{\left[1 + \left(G_{max} / \tau_{max_oct} \right) |\gamma_{e_oct}| \right]^2} \quad (2)$$

where G_{max} is the initial shear modulus, τ_{max_oct} is the maximum octahedral shear stress in three dimensional state which is related to shear parameters of soil through cohesion c and internal angle of friction ϕ , and γ_{e_oct} is the octahedral shear strain. The tangent modulus during unloading/reloading cycle is

$$G_t = \frac{G_{max}}{\left[1 + \left(G_{max} / 2\tau_{max_oct} \right) |\Delta\gamma_{oct}| \right]^2} \quad (3)$$

where $\Delta\gamma_{oct}$ represent the difference in octahedral shear strain during unloading/reloading cycle. In unloading case as it equals to $(\gamma_{e_oct} - \gamma_{u_oct})$ and in reloading case it is $(\gamma_{e_oct} - \gamma_{r_oct})$. γ_{e_oct} is the octahedral shear strain at present state and γ_{u_oct} and

are octahedral shear strains at starting points of unloading and reloading, respectively, for that cycle.

Reinforcement material

The geotextile reinforcements are modelled using the geogrid structural element in FLAC^{3D}. The geogrid elements are three noded shell elements that resist as membrane but do not resist bending loading. The geogrid element behaves as isotropic linear elastic material with no failure limit. The effective confining stress and total shear stress developed on geogrid are balanced by the membrane stress developed within the geogrid itself (Itasca, 2008). The required input parameters for geogrid element in FLAC^{3D} are: (1) elastic modulus (2) Poisson's ratio (3) thickness of geogrid.

Interface Properties

The interfaces between the dissimilar materials are modelled as linear spring-slider system. The interface between the soil and reinforcement are numerically modelled in this simulation. The interface behavior of geogrid is represented numerically at each geogrid node by a rigid attachment in normal direction and spring-slider in the tangent plane to the geogrid surface (Itasca, 2008). The required input parameters for interaction between geogrid and FLAC^{3D} grid are : (1) coupling spring cohesion (2) coupling spring friction (3) coupling spring stiffness. The model material properties adopted by Bhattacharjee and Krishna (2012) are used in the simulation (Table 1).

Failure ratio	0.9
Dilation angle, Degrees	15
Reinforcement (Geotextile) properties	
Mass density, kg/m ³	0.23
Thickness, m	0.001
Stiffness, kN/m	25,75,150
Reinforcement (Geotextile) interface properties	
Coupling spring cohesion, kPa	0.1
Coupling spring friction, Degrees	30
Coupling spring stiffness, kPa	1×10 ⁶

Boundary condition

The bottom boundaries are completely fixed in vertical direction. The far end boundaries are fixed in x direction during construction. During the construction the model wall is fixed in horizontal direction to represent the facing support. The lateral boundaries are fixed in y direction to represent the lateral boundaries. After the completion of construction of all layers the model is brought to equilibrium. Then the facing boundaries are removed stage by stage representing the stage wise removal of support. After the support removal the model is brought to equilibrium.

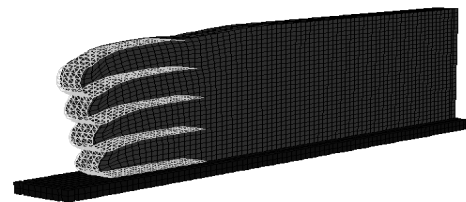


FIG. 2 DISPLACED GRID AFTER DYNAMIC EXCITATION

The constitutive model for soil is able to implement the damping of soil through the cyclic hysteresis. However, local damping ratio of 5% is adopted for soil element during dynamic analysis to simulate the properly the damping of soil when strain level is small (Liu et al. 2011). The sinusoidal dynamic excitation of 0.2g input acceleration and 5Hz frequency is applied at the stiff bottom in the form of wave velocity in horizontal direction (uni-axial shaking). The displaced grid after dynamic excitation is shown in Fig. 2.

TABLE I

MATERIAL PROPERTIES IN NUMERICAL MODEL

Soil properties for Mohr model with hyperbolic soil parameters (Duncan et. al, 1980)	
Mass density, kg/m ³	1630
Elastic modulus, kPa	1×10 ⁴
Poisson's ratio	0.3
Friction angles, degrees	
Dilation angle, degree	
Cohesion, kPa	0.1
Atmospheric pressure kPa	101.3
Modulus number	1660
Modulus exponent	0.678

IV. RESULT AND DISCUSSION

Effect of Backfill Friction Angle

The horizontal displacements and vertical displacements are observed at different elevations at face of wall (at 0.5m from face of wall), at the end of reinforcement (at 4.25m from face of wall) and at the deep backfill (at 14.0 m from face of wall) and is shown in Fig. 3. The horizontal displacements are maximum at the face of wall. The horizontal displacements decrease as the distance from face increases and at deep backfill it is almost negligible.

The horizontal displacements are maximum for wall with loose backfill ($\phi = 30^\circ$) for both face of wall and end of reinforcement. The horizontal displacements at higher backfill friction angle ($\phi = 38^\circ$ and 43°) are almost equal. The vertical displacements near the end of reinforcement are more than that of face of wall. This signifies settlement near the end of reinforcement. The vertical displacements are also more for wall with loose backfill ($\phi = 30^\circ$). The octahedral shear strain, horizontal displacement and vertical displacements along the length of backfill are presented in Fig. 4 & 5 for backfill friction angle of 38° and 30° . From the Fig. 4 it is observed that the horizontal displacements of soil element within reinforced zone are maximum and they decrease gradually and become negligible after end of reinforcement at elevation of 5.7 m, 4.8 m, and 3.6 m. But at the lower layers i.e 2.4 m and 1.2 m the horizontal movement of soil element decreases to zero within reinforced zone. The vertical settlements are almost uniform within reinforced zone i.e up to a distance of 4 m from wall facing at an elevation of 5.7 m, 4.8 m and 3.6 m. The vertical settlement increases suddenly near the end of reinforcement at higher layers i.e at an elevation of 5.7 m, 4.8 m and 3.6 m. The vertical settlements are lesser at lower layers i.e at an elevation of 2.4 m and 1.2 m and decreases to zero within reinforced zone. The octahedral shear strain reaches peak within reinforced zone near end of reinforcement within reinforced zone and after end of reinforcement in backfill soil. By comparing the octahedral shear strain, horizontal displacement and vertical settlement at different layers, it can be seen that the deformation of wrap faced wall subjected to dynamic excitation consist of three different modes: shear deformation within reinforced zone, relative compaction near end of reinforcement and shear zone extending to backfill zone.

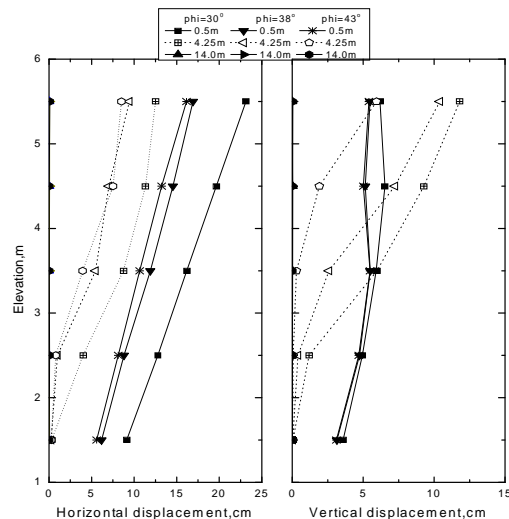


FIG.3 HORIZONTAL AND VERTICAL DISPLACEMENT FOR DIFFERENT BACKFILL FRICTION ANGLE ($\phi = 30^\circ, 38^\circ$ AND 43°) AFTER AFTER 20 CYCLES OF DYNAMIC EXCITATION OF 0.2G AND 5HZ ($L_{REIN}/H=0.7$, NO. OF REINFORCEMENT LAYERS=6)

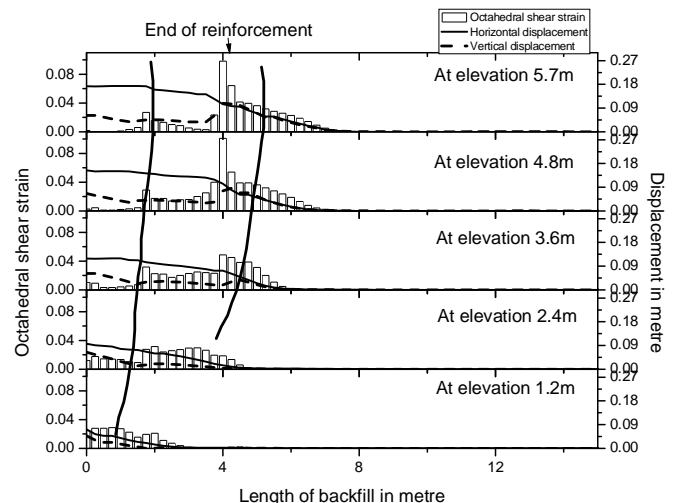


FIG. 4 OCTAHEDRAL SHEAR STRAIN, HORIZONTAL DISPLACEMENT AND VERTICAL DISPLACEMENT ALONG THE LENGTH OF BACKFILL AFTER 20 CYCLES OF DYNAMIC EXCITATION OF 0.2G AND 5HZ ($\phi = 38^\circ, L_{REIN}/H=0.7$, NO. OF REINFORCEMENT LAYERS=6, $\psi = 10^\circ$)

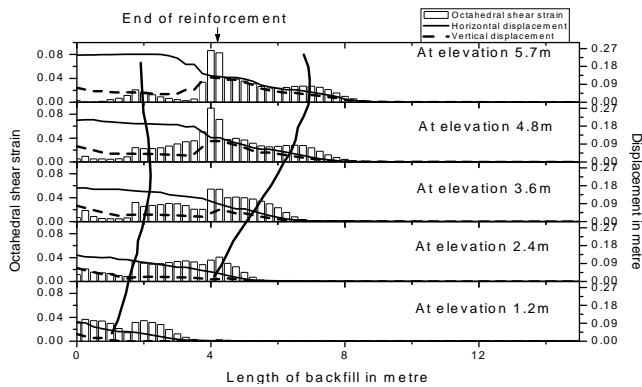


FIG. 5 OCTAHEDRAL SHEAR STRAIN, HORIZONTAL DISPLACEMENT AND VERTICAL DISPLACEMENT ALONG THE LENGTH OF BACKFILL AFTER 20 CYCLES OF DYNAMIC EXCITATION OF 0.2G AND 5HZ ($\phi = 30^\circ$, $L_{REIN}/H=0.7$, NO. OF REINFORCEMENT LAYERS=6, $\Psi = 10^\circ$)

By comparing Fig.4 and 5, it is observed that the more horizontal displacements and vertical displacements of backfill soil after the end of reinforcement for soil having $\phi = 30^\circ$. The octahedral shear strains are also extended more into the backfill for soil having $\phi = 30^\circ$. The shear zone extends more into the deep backfill for soil having $\phi = 30^\circ$. Three modes of deformations shear deformation within reinforced zone, relative compaction near end of reinforcement and shear zone extending to backfill zone are observed for wall with $\phi = 30^\circ$, with more extended shear zone into the backfill soil.

Effect of Dilation Angle

The horizontal displacements and vertical displacements are observed at different elevations at face of wall (at 0.5m from face of wall), at the end of reinforcement (at 4.25m from face of wall) and at the deep backfill (at 14.0 m from face of wall) for different dilation angle and is shown in Fig. 6. The horizontal displacements are maximum at the face of wall. The horizontal displacements decrease as the distance from face of increases and at deep backfill it is almost negligible. The horizontal displacement and vertical displacement at wall is maximum for wall with lowest dilation angle. The vertical displacements are more near end of reinforcements.

The octahedral shear strain, horizontal displacement and vertical displacements along the length of backfill are presented in Fig. 7 and 8 for backfill dilation angle of 5° and 15° . The octahedral shear strain is extended deep

into the backfill with dilation angle 5° . The octahedral strain on soil is more for soil with 5° dilation angle. But octahedral shear strain within the reinforced is very low for soil with 15° dilation angle. The horizontal and vertical displacement shows similar trend for soil with dilation angle 5° , 10° and 15° . The vertical displacement increases near the end of reinforcement for all three cases indicating vertical settlement near the end of reinforcement. The all three modes of failure is prominent near for wall with backfill soil having 5° and 10° dilation angle. But the shear deformation within reinforced zone may not form at higher layers of backfill soil for soil with dilation angle 15° .

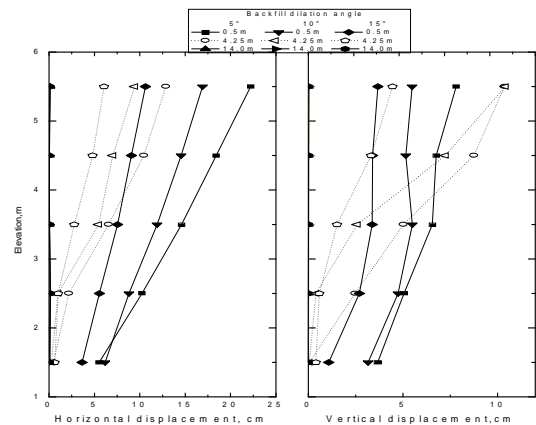


FIG.6 HORIZONTAL AND VERTICAL DISPLACEMENT FOR DIFFERENT BACKFILL DILATION ANGLE ($\Psi = 5^\circ, 10^\circ$ AND 15°) AFTER AFTER 20 CYCLES OF DYNAMIC EXCITATION OF 0.2G AND 5HZ ($\phi = 38^\circ$, $L_{REIN}/H=0.7$, NO. OF REINFORCEMENT LAYERS=6)

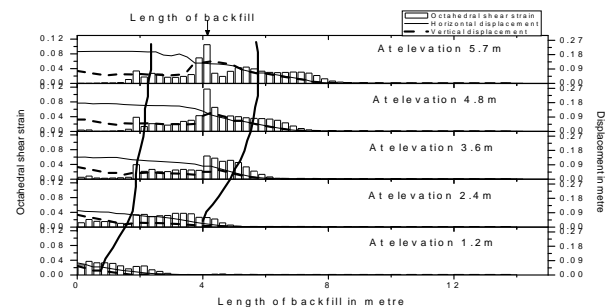


FIG. 7 OCTAHEDRAL SHEAR STRAIN, HORIZONTAL DISPLACEMENT AND VERTICAL DISPLACEMENT ALONG THE LENGTH OF BACKFILL AFTER 20 CYCLES OF DYNAMIC EXCITATION OF 0.2G AND 5HZ ($\phi = 38^\circ$, $L_{REIN}/H=0.7$, NO. OF REINFORCEMENT LAYERS=6, $\Psi = 5^\circ$)

V. CONCLUSIONS

The following observations are made from the present study:

1. The deformation of wrap faced reinforced soil wall is due to three distinct modes of failure surfaces – shear deformation within reinforced zone, relative compaction near end of reinforcement and compound failure surface extending to backfill zone.

2. The backfill friction angle effects the deformation due to shear zone extending to the backfill. The wall with higher friction angle have shear zone but near the end of reinforcement, while wall with lower friction angle the shear zone extend deep into the backfill.

3. The backfill dilation angle effects the deformation due to shear zone extending to the backfill. The wall with higher dilation angle have shear zone but near the end of reinforcement.

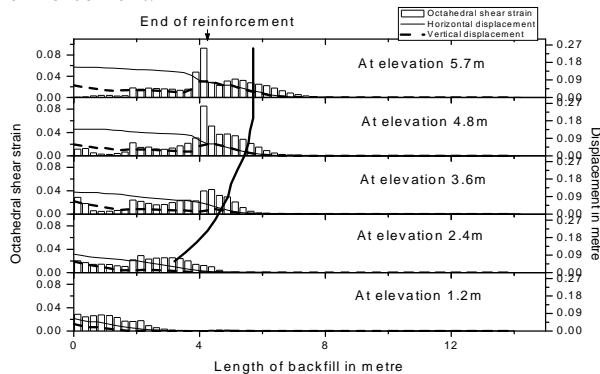


FIG. 8 OCTAHEDRAL SHEAR STRAIN, HORIZONTAL DISPLACEMENT AND VERTICAL DISPLACEMENT ALONG THE LENGTH OF BACKFILL AFTER 20 CYCLES OF DYNAMIC

EXCITATION OF 0.2G AND 5 HZ ($\Phi = 38^\circ$, $L_{REIN}/H=0.7$, NO. OF REINFORCEMENT LAYERS=6, $\Psi = 15^\circ$)

REFERENCES

- [1] K.Hatami, R.J.Bathurst (2000). Effect of structural design on fundamental frequency of reinforced-soil retaining walls. *Soil Dynamics and Earthquake Engineering*, 19(2000), 137-157.
- [2] H.I. Ling, S.Yang, D.Leshchinsky, H.Liu and C.Burke(2010). Finite-element simulations of full scale modular-block reinforced soil retaining walls under earthquake loading. *Journal of Engineering Mechanics*, ASCE, Vol. 136, No. 5,653-661.
- [3] H.Liu and H.I.Ling (2011). Seismic response of reinforced soil retaining walls and strain-softening of backfill soil. *International Journal of Geomechanics*, ASCE, doi:10.1061/(ASCE)GM.1943-5622.0000051.
- [4] H.Liu, X.Wang and E.Song (2011). Reinforcement load and deformation mode of geosynthetics-reinforced soil walls subject to seismic loading during service life. *Geotextiles and Geomembranes*, 29,1-16.
- [5] A.M.Krishna and G.M.Latha (2012). Modeling of dynamic response of wrap faced reinforced soil retaining wall. *International Journal of Geomechanics*, ASCE, Vol.12, No.4, doi:10.1061/(ASCE)GM.1943-5622.0000128.
- [6] A.Bhattacharjee, and A.M.Krishna (2012). Development of numerical model for wrap-faced walls subjected to seismic excitation, *Geosynthetic International*, 19, No.5, 1-16.
- [7] R.L.Kuhlemeyer and J.Lysmer (1973). Finite element method accuracy for wave propagation problems, *Journal Soil Mechanics and Foundations Div. ASCE*, Vol. 99, No. SM5, 421-427.
- [8] J.M.Duncan, P.Byrne, S.K.Wong. and P.Mabry (1980). Strength, stress, strain and bulk modulus parameters for finite element analyses of stresses and movements in soil masses. Report No. UCB/GT/80-01, Department of Civil Engineering, University of California, Berkeley.
- [9] K.Hatami and R.J.Bathurst (2005). Development and verification of a numerical model for the analysis of geosynthetic-reinforced soil segmental walls under working stress conditions. *Canadian Geotechnical Journal*, Vol. 42, No. 4,1066-1085.